| | | |
|---|---|---|
| ESRF | **Experiment title:**<br>The interaction of Langmuir monolayers with viral fusion peptides of classes I-III | **Experiment number**:<br>SC-4684 |
| **Beamline**:<br>ID10 | **Date of experiment**:<br>from: 15.02.2018 to: 18.02.2018 | **Date of report**:<br>05.03.2018 |
| **Shifts:**<br>9 | **Local contact(s)**:<br>Oleg Konovalov | *Received at ESRF:* |

**Names and affiliations of applicants** (* indicates experimentalists):

Göran Surmeier*[1], Susanne Dogan*[1], Christian Albers*[1], Simon Egger*[2], Michael Paulus*[1], Metin Tolan[1], Julia Nase*[1],

**[1] Fakultät Physik / DELTA, Technische Universität Dortmund, 44221 Dortmund, Germany**

**[2] Fakultät Chemie, Technische Universität Dortmund, 44221 Dortmund, Germany**

## Report:

We conducted a combined grazing incidence diffraction (GID) and X-ray reflectivity (XRR) study on the interaction of viral fusion peptides (FP) with lipid monolayers at the air-water interface. Viral fusion peptides are segments of viral fusion proteins located in the ectodomain exposed to the external aqueous medium. They have membrane perturbing properties leading to the opening of fusion pores and thereby initiating the fusion process, when a virus enters a host cell.

We spread the phospholipid 1,2-dipalmitoyl-*sn*-glycero-3-phosphocholine (DPPC) on the surface of a phosphate buffer subphase at pH 5 in a Langmuir trough to obtain a well-arranged monolayer. The fusion peptides were dissolved in 1 ml buffer and then injected underneath the monolayer, resulting in a final peptide concentration of 2 µM. We studied four different fusogenic peptides. The class I fusion peptide of Hemagglutinin 2 (HA2), the class II fusion peptide of Tick-borne encephalitis virus (TBEV), the class III fusion peptide of vesicular stomatitis virus (VSV) and the transmembrane domain (TMD) of VSV. The TMD is a peptide sequence that plays an important role in the stabilization of fusion pores at a later stage of membrane fusion. The peptides were added at surface pressures of the DPPC film of 5, 15, and 35 mN/m. XRR and GID scans were performed before and after the injection at a photon energy of 22 keV. During the experiments, the sample environment was flushed with helium in order to suppress air scattering and to prevent oxidative beam damage.

It emerged that HA2 has the strongest effect on the DPPC Langmuir layer. As soon as it is injected underneath the membrane, the surface pressure increases up to a saturation value of approximately 27 mN/m, independent of the initial value. At an injection pressure of 5 mN/m, adding HA2 leads to a phase transition of the membrane from the liquid-expanded to the liquid-condensed phase, which is indicated by the fact that the lateral structural reflexes in the GID patterns are only formed after the peptide has been added. At a starting pressure of 15 mN/m, we observed that the lattice constants drop from 5.81 Å and 5.19 Å ($\gamma$=56.0°) to 5.66 Å and 5.14 Å ($\gamma$=56.5°) and the tilt angle decreases from 36.3° to 33.5°. The corresponding GID patterns are shown in *figure 1*. Adding HA2 at 35 mN/m, which is a higher surface pressure than the saturation value, does not seem to affect the membrane parameters. Preliminary results of a GID

measurement series including all peptides can be found in *table 1*. A more detailed data analysis and the evaluation of the reflectivity curves is still in progress.

Our results indicate that the hydrophobic effect alone is insufficient to trigger the peptide-membrane interaction for classes II and III and the TMD. In contrast to HA2, these peptides are polycationic, thus, their insertion or respectively adsorption behaviour is expected to depend more strongly on the electrostatic properties of the target membrane. In order to obtain an exhaustive picture, electrostatic interactions have to be considered. Therefore, we plan to complete our dataset by studying an anionic Langmuir monolayer consisting of 1,2-Dipalmitoyl-*sn*-glycero-3-phosphatidic acid (DPPA). The comparative measurements on the charged membrane will be an important contribution to a valid data interpretation.

**Acknowledgements**: This work is supported by the Forschergruppe 1979 (**DFG-FOR1979**). Also, we acknowledge our local contact Dr. Oleg Konovalov and the ID10 staff for the assistance during our experiment.

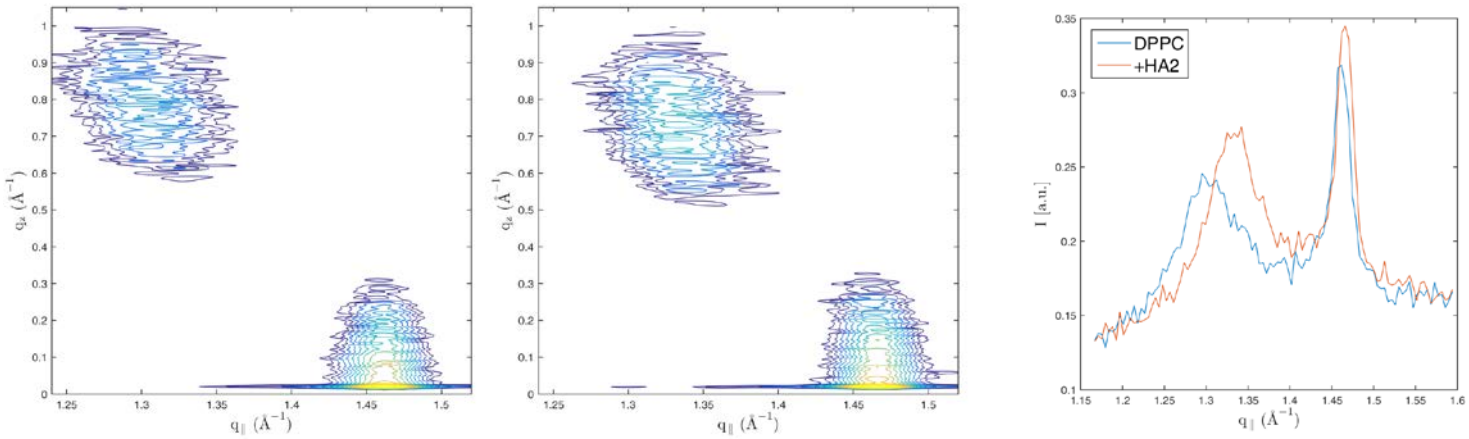


*Figure 1*: GID patterns of a DPPC monolayer at 15 mN/m before (left) and after (center) the injection of HA2 and the corresponding data integrated in the $q_z$ direction (right).

*Table 1*: Lattice Parameters for DPPC Monolayers in absence and presence of fusogenic peptides extracted from GID patterns. Documented are the lattice constants *a*, *b* and the included angle $\gamma$, the area per lipid *A*, the azimuthal and polar tilt agles $\theta$ and $\tau$ and crystallite size *L* along *a*.

| | $\pi$ (mN/m) | *a* (Å) | *b* (Å) | $\gamma$ (°) | *A* (Å$^2$) | $\theta$ (°) | $\tau$ (°) | *L* (Å) |
|---|---|---|---|---|---|---|---|---|
| DPPC | 5 | *No Bragg reflections observed.* | | | | | | |
| +HA2-FP | | 5.71 | 5.15 | 56.4 | 24.49 | 56.4 | 34.3 | 379 |
| DPPC | 15 | 5.81 | 5.18 | 56.0 | 24.97 | 56.0 | 36.3 | 441 |
| +HA2-FP | | 5.66 | 5.14 | 56.6 | 24.29 | 56.6 | 33.5 | 461 |
| DPPC | 35 | 5.52 | 5.09 | 57.2 | 23.58 | 57.2 | 31.1 | 474 |
| +HA2-FP | | 5.50 | 5.08 | 57.2 | 23.52 | 57.2 | 30.9 | 450 |
| DPPC | 5 | *No Bragg reflections observed.* | | | | | | |
| +TBEV-FP | | *No Bragg reflections observed.* | | | | | | |
| DPPC | 15 | 5.80 | 5.18 | 56.0 | 24.95 | 56 | 36.8 | 487 |
| +TBEV-FP | | 5.88 | 5.21 | 55.7 | 25.30 | 55.7 | 37.4 | 482 |
| DPPC | 35 | 5.54 | 5.09 | 57.1 | 23.67 | 57.1 | 31.8 | 521 |
| +TBEV-FP | | 5.50 | 5.08 | 57.2 | 23.52 | 57.2 | 31.8 | 516 |
| DPPC | 5 | *No Bragg reflections observed.* | | | | | | |
| +VSV-FP | | *No Bragg reflections observed.* | | | | | | |
| DPPC | 15 | 5.80 | 5.19 | 56.0 | 24.96 | 56.0 | 36.4 | 468 |
| +VSV-FP | | 5.84 | 5.20 | 55.8 | 25.08 | 55.8 | 36.5 | 496 |
| DPPC | 35 | 5.52 | 5.09 | 57.2 | 23.57 | 57.2 | 31.1 | 478 |
| +VSV-FP | | 5.51 | 5.08 | 57.2 | 23.54 | 57.2 | 31.5 | 470 |
| DPPC | 5 | *No Bragg reflections observed.* | | | | | | |
| +VSV-TMD | | *No Bragg reflections observed.* | | | | | | |
| DPPC | 15 | 5.82 | 5.19 | 55.9 | 25.04 | 55.9 | 36.5 | 465 |
| +VSV-TMD | | 5.84 | 5.20 | 55.8 | 25.12 | 55.8 | 36.5 | 468 |
| DPPC | 35 | 5.54 | 5.09 | 57.1 | 23.67 | 57.1 | 31.2 | 507 |
| +VSV-TMD | | 5.54 | 5.09 | 57.1 | 23.69 | 57.1 | 32.0 | 505 |